Analyst

Accepted Manuscript

This article can be cited before page numbers have been issued, to do this please use: A. T. George, A. M. MS, P. Srivasatava, S. Sunil, V. V. R. Sai and R. Srinivasan, *Analyst*, 2020, DOI: 10.1039/D0AN01603A.

ROYAL SOCIETY OF CHEMISTRY

rsc.li/analyst

View Article Online
DOI: 10.1039/D0AN01603A

ARTICLE

Development of U-bent plastic optical fiber biosensor with plasmonic labels for detection of chikungunya non-structural protein 3

Ankitha George[a], M S Amrutha[a], Priyanshu Srivastava[b], Sujatha Sunil[b*], V. V. R. Sai[c*], Ramanathan Srinivasan[d*]

Received 00th January 20xx,
Accepted 00th January 20xx

DOI: 10.1039/x0xx00000x

This study presents a novel plasmonic fiber optic sandwich immunobiosensor for the detection of chikungunya, an infectious mosquito-borne disease with chronic musculoskeletal pain and acute febrile illness, by exploiting non-structural protein 3 (CHIKV-nsP3) as a biomarker. A plasmonic sandwich immunoassay for CHIKV-nsP3 was realized on the surface of a compact U-bent plastic optical fiber (POF, 0.5 mm core diameter) with gold nanoparticles (AuNP) as labels. High evanescent wave absorbance (EWA) sensitivity of the U-bent probes allows absorption of the light passing through the fiber by the AuNP labels, upon the formation of sandwich immunocomplex of CHIKV-nsP3 on the core surface of the U-bent probe region. A simple optical set-up with a low-cost green LED and a photodetector on its either end of the U-bent probe gave rise to a detection limit of 0.52 ng/mL (8.6 pM), and a linear range of 1 – 10^4 ng/mL with a sensitivity of 0.1043 $A_{530\ nm}/\log(C_{nsP3})$. In addition, the plasmonic POF biosensor shows strong specificity towards CHIKV-nsP3 analyte in comparison to Pf-HRP2, HIgG, and Dengue whole virus. The results illustrate the potential of plasmonic POF biosensors for direct and sensitive point-of-care detection of chikungunya viral disease.

Introduction

Biosensors are analytical devices that use state of the art technology with various biological entities to find applications in a variety of fields, especially disease diagnosis [1, 2]. The integration of extreme specificity and sensitivity of bioaffinity molecules and the physiochemical transducers to provide sophisticated and accurate bioanalytical results paved the way for the development and further research of handy and straightforward portable diagnostic devices [3]. The biosensors can be developed either as label-free or labeled, in which the former generates signals directly when the biorecognition event takes place [4, 5]. The latter one requires an external element physically or chemically attached to the biomolecule of interest, which will generate or amplify the signal due to additional interactions [6]. Biosensors employ micro and nanofabrication techniques with various sensing strategies like electrochemical, optical, piezoelectric, or magnetic methods [7],

[a]*Department of Chemical Engineering, Indian Institute of Technology, Madras, India*
[b]*International Centre for Genetic Engineering and Biotechnology, Delhi, India*
cDepartment of Applied Mechanics, Indian Institute of Technology, Madras, India
† Footnotes relating to the title and/or authors should appear here.
Electronic Supplementary Information (ESI) available: [details of any supplementary information available should be included here]. See DOI: 10.1039/x0xx00000x

and have shown potential to be utilized for early and fast diagnosis of deadly infectious diseases, including vector-borne diseases [8].

Chikungunya is amongst the major mosquito-borne diseases that are responsible for lifelong disabilities owing to rheumatoid and neurological complications it inflicts on the affected individuals [9]. Currently, the diagnosis of this viral infection is deficient due to overlapping clinical symptoms with other diseases such as dengue and zika [10, 11]. Detection of antibodies against the chikungunya virus (CHIKV) is still the preferred way of diagnosis, and several recent attempts have been made to detect CHIKV antigens in patient samples [12, 13]. For this purpose, several viral proteins have been utilized, such as the envelope proteins, namely, CHIKV E1 and E2 [12, 14], and non-structural protein 3 (CHIKV-nsP3) [13, 15, 16]. Similarly, immuno-chromatographic tests and biosensing have also been employed to detect antigens with varying success rates [13, 14, 16-18]. Amongst these methods, biosensing schemes are gaining popularity owing to the ease of techniques and portability of the assays as point-of-care diagnostics with limited expertise and infrastructure [13, 17, 18].

Fiber-optic biosensors based on evanescent wave absorbance, especially the U-bent fiber optic sensor probes in combination with plasmonic nanomaterials, offer several advantages, including dipping or drop-casting of samples for biochemical reactions, rapid and real-time response and improved analyte detection limits with more straightforward optoelectronic instrumentation [19, 20]. The sensing mechanism is based on the evanescent wave (EW) at the core-medium interface of a decladded fiber, which is an exponentially decaying fraction of light, penetrating the optically thinner medium during the total internal reflection [21, 22]. While the intensity of EW depends on the refractive index (RI) of the adjacent medium, the light propagating through the fiber can undergo attenuation upon the presence of optically active elements (e.g., a chromophore) within the EW field. The optical absorption through the U-bent probe is directly proportional to the number of the chromophores and their extinction coefficient. It can be monitored in real-time [23, 24]. Lately, plastic optical fibers (POF) are being considered as a better replacement to conventional silica fibers in view of their handiness, flexibility, and ease of machinability [25-27], and compared to straight probes, U-bent geometry in optical fibers has proven to provide a significant improvement in absorbance sensitivity [28-32]. The multimode fibers typically employed in the construction of U-bent probes allow the use of a pair of a simple LED and a photodetector to couple light into the fiber and measure the optical losses, respectively [21, 29, 33, 34]. Fiber probes with suitable modifications can be used for the detection of biological and environmental samples, with an excellent limit of detection (LOD) [35, 36].

In this work, we have developed a U-bent POF based biosensor with plasmonic labels to detect CHIKV-nsP3. To the best of our knowledge, this is the first report of the detection of CHIKV antigen using an optical transduction method. A labeled sandwich immunoassay was established using the POFs, in which the target analytes were introduced to optical fiber surface-immobilized with the primary antibody, and the resulting antibody-antigen complex is captured with a secondary antibody conjugated with gold nanoparticles (AuNP). AuNP were used as the labels on account of their higher extinction coefficient than that of conventional labels, the ability to conjugate biomolecules, and their tunable size and shape [37-39]. The LOD, sensitivity, and specificity of the developed immunosensors were evaluated. The surface morphological changes after performing sandwich immunoassay were characterized using scanning electron microscopy (SEM).

Experimental

Materials and reagents

Super ESKATM plastic optical fibers of 250 and 500 µm (SK 10 and SK 20, respectively) were purchased from Keiko Corporation, Japan. Sulphuric acid (H_2SO_4), hexamethylene diamine (HMDA), gold (III) chloride ($HAuCl_4$), sodium citrate dihydrate, sodium hydroxide (NaOH), thiolated polyethylene glycol (SH-PEG, M.W 6000 Da), Monoclonal anti-polyhistidine antibody, phosphate buffer saline (PBS) and bovine serum albumin (BSA) were procured from Sigma Aldrich, India. Glutaraldehyde was purchased from Fluka. All chemicals used in the experiments were of analytical grade. Milli-Q water (18.2 MΩ.cm at 25 °C, from Millipore) was used in all the experiments.

Fabrication of U-bent POF probes

The core and cladding of the POF are made of polymethyl methacrylate (PMMA) and a fluorinated polymer with a refractive index of 1.49 and 1.41, respectively. The U-bent POF probes were made as described elsewhere [26]. Briefly, a 25 cm long 250 and 500 µm POF bent at the middle portion, were inserted into capillary glass tubes of 1 and 1.75 mm diameter, respectively. The capillaries were sealed with scotch tape and heated at 95 °C for 10 min, to obtain U-bent probes with 0.75 and 1.5 mm bend diameters, respectively. The U-bent region was decladded through chemical etching by incubating the probes in ethyl acetate for 2 minutes. The variations between the probes were minimized by carefully choosing the probes with RI sensitivity around 3.404 ± 0.11 A530 nm/RIU for further analysis. The RI sensitivity was verified by exposing the POFs to sucrose solutions of various concentrations, as described elsewhere [26].

Surface functionalization

View Article Online
DOI: 10.1039/D0AN01603A

The decladded surface was pretreated by rinsing the fiber probe with ethanol and then thoroughly washing with de-ionized water (DI). The cleaned U-bent probe surface was then exposed to 1 M H_2SO_4 for 5 minutes. This step is necessary to obtain carboxylic groups on the PMMA surface by the reduction of the methyl ester groups via acid hydrolysis [40]. Then amine functional groups were generated on the surface by incubating the probes in 10% hexamethylene diamine (HMDA) solution in 100 mM borate buffer for two hours at room temperature. The pH of the buffer was 11.5. After rinsing thoroughly with DI water, the probes were exposed to 2.5% glutaraldehyde for 30 minutes.

Immobilization of primary antibodies

The anti-polyhistidine monoclonal antibody was used as the primary (receptor) antibody to capture the CHIKV-nsP3 protein through the histidine tags at its N-terminus. The glutaraldehyde functionalized fiber surface was incubated in 100 µg/mL of primary antibody diluted in 10 mM PBS, and stored overnight at 4 °C. The biorecognition molecules were attached to the aldehyde functionalized probe surface through their amine groups via Schiff's base links [41]. Subsequently, the probes were thoroughly washed with PBS and incubated in 5 mg/mL BSA for 30 minutes to block unbound sites.

Gold nanoparticle synthesis and conjugation with capture antibodies

Anti-CHIKVnsP3 polyclonal antibody (CHIKV-nsP3Ab) was used as the detection antibody to perform the sandwich immunoassay with 40 nm AuNP as labels. The purification and isolation of CHIKV-nsP3 analyte and anti-CHIKVnsP3 antibody were carried out as per the procedures described elsewhere [13]. The AuNP of specific size were prepared in our lab as per the protocol described by Turkevich et al. [42]. Briefly, 200 µL of 0.05 M $AuCl_3$ solution was added to 39.15 mL of DI water, and this solution was heated. As soon as boiling commenced, 0.647 mL of 5 mg/mL sodium citrate trihydrate solution was added. The heating was continued until the solution color changed to pale purple. Subsequently, the solution was allowed to cool to room temperature. The absorbance spectra of the synthesized AuNP solution was recorded using a UV-vis spectrophotometer, and the maximum absorbance peak was observed at 529 nm.

The concentration of CHIKV-nsP3Ab for conjugation was optimized, as described in section '**AuNP bioconjugation with anti-CHIKV-nsP3 antibodies'**. For conjugation, 100 µl of CHIKV-nsP3Ab at an optimum concentration was added to 1 mL of 40 nm AuNP (pH adjusted to 8.5) and incubated for 30 minutes. Subsequently, the unbound surface was blocked using 80 µl of 320 µM SH-PEG for 15 minutes to avoid any non – specific binding. Then the solution was centrifuged at 7000 rpm for 25 minutes to remove the excess antibodies. The process was repeated thrice, and the final AuNP solution conjugated with CHIKV-nsP3Ab (AuNP-CHIKVnsP3Ab) was resuspended in PBS to 100 µL volume. The solution was kept at 4 °C until further use.

Optical set up

In halogen-lamp based biosensor set up, power level drifts can be a serious issue. With the advent of LEDs, the drift is not significant, and hence we employed a green LED source to mitigate this issue. The optical fiber probes were connected to a green LED light source (M530F2, 200 mA, Thorlabs Inc., USA) driven by a steady current supply, and an optical power meter (PM100USB, Thorlabs Inc., USA) at either of its ends using a multimode SMA905 connector and bare fiber terminator (BFT1) (Thorlabs Inc., USA). The absorbance was measured with an integration time of 1 ms, and values reported are the average of 3000 samples.

Direct and Sandwich immunoassay

To perform a direct assay, i.e., without using a primary antibody, the aldehyde treated fiber probes were incubated in 10 µg/mL CHIKV-nsP3 and left overnight at 4 ˚C. Subsequently, the probes were thoroughly washed in PBS before incubating them in 5 mg/mL BSA for ~30 minutes to block the free aldehyde groups on the surface. The real-time absorbance change on the adsorption of AuNP-CHIKVnsP3Ab to the analyte bound probe was recorded.

In sandwich immunoassay, a monoclonal anti-polyhistidine antibody was used as the bioreceptor (primary antibody) immobilized on the probe surface. CHIKV-nsP3 and AuNP-CHIKVnsP3Ab were used as the detection analyte and labeled secondary antibody, respectively. The U-bent probe surface was exposed to 30 µL of each sample taken in a 200 µL cell, and the real-time absorbance change was monitored as portrayed in the pictorial shown in Figure 1. After incubating in CHIKV-nsP3 for ~ 2 hrs, the biofunctionalized surfaces were exposed to AuNP-CHIKVnsP3Ab for ~ 1.5 hrs. The sensitivity and LOD of the sensor using sandwich immunoassay were assessed by analyzing samples with different concentrations of CHIKV-nsP3 analyte. A separate probe was employed for each concentration of the analyte. Control experiments were carried out by incubating the biofunctionalized probe directly on to AuNP-CHIKVnsP3Ab, i.e., without exposing the probe to the analyte. All the experiments were repeated three times, and the average and standard deviations are presented.

Surface characterization

The morphological changes from the bare probe to AuNP-CHIKVnsP3Ab adsorbed fiber were evaluated using SEM analysis (S4800 SEM, Hitachi, Japan). An acceleration voltage of 5 keV was used in the SEM analysis.

Specificity analysis

An ideal biosensor should have the ability to specifically quantify the analyte of interest while yielding little or no signal when exposed to other biomolecules [33]. In order to analyze the specificity

View Article Online
DOI: 10.1039/D0AN01603A

of the fiber optic immunosensor towards CHIKV-nsP3, it was exposed to different bio-analytes such as human immunoglobulin (HIgG), histidine-rich protein II of Plasmodium falciparum (Pf-HRP2) and dengue virus (DENV), and the absorbance changes were compared with that of probes exposed to CHIKV-nsP3.

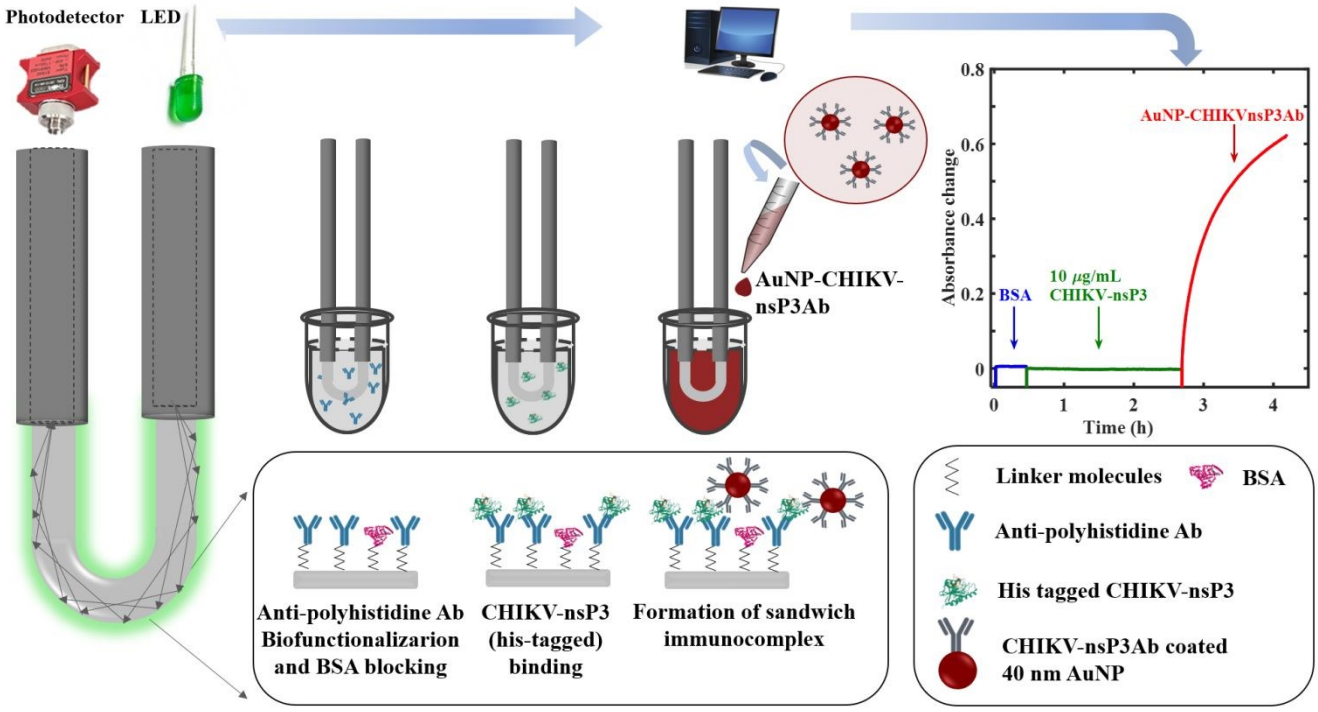

Figure 1. Pictorial (not drawn to scale) showing the components of U-bent fiber optic immunosensor for CHIKV-nsP3 detection. The sandwich assay was realized using AuNP labeled CHIKV-nsP3Ab (AuNP-CHIKVnsP3Ab). One terminal of the probe is connected to a light source, and the other end is connected to a spectrometer or photodetector.

Results and Discussions

Earlier studies reveal that U-bent POF probes with a fiber core diameter less than 1000 µm and a bend diameter equal to thrice that of fiber core are optimum for highest refractive index sensitivity [26, 43]. In order to identify the optimum POF diameter for the biosensing, U-bent probes fabricated using 250, and 500 µm POFs were evaluated using a model analyte. Human immunoglobulin G (HIgG) was chosen as the model analyte, and a plasmonic sandwich assay with HIgG was realized using POFs of different diameters. The HIgG detection results are described in the following section. Subsequently, POFs with the optimal diameter were used in CHIKV-nsP3 detection.

Optimum U-bent POF probe geometry for biosensing

Here, Goat anti-Human IgG (GaHIgG) antibodies that are specific to fragment antigen-binding (Fab) and fragment crystallizable (Fc) regions of HIgG were used respectively as the capture and detection antibodies. The capture antibodies were immobilized on the aldehyde functionalized U-bent probes, as described earlier. The AuNP conjugated with 25 µg/mL Fc-GaHIgG (Gabs) was obtained as per the procedure reported elsewhere [37].

A plasmonic sandwich immunoassay was realized on U-bent probes made of 250 and 500 µm using LED and PD set up, as shown in Figure 2 (a) and (b), respectively, and the absorbance response was monitored in real-time. The Fab-GaHIgG immobilized U-bent probes were exposed to BSA solution for 15 minutes to minimize any non-specific binding. Then, the probes were incubated in the Gabs solution for 20 minutes to investigate the non-specific adsorption of Gabs to the BSA coated probe surface. There was no considerable increase in the absorbance at 540 nm, indicating negligible adsorption of Gabs to the sensor surface. Subsequently, a sandwich immunocomplex formation on the U-bent probes was realized by incubating the probes in 1 µg/mL HIgG and Gabs for ~ 1 hour and ~ 30 minutes, respectively. An average absorbance

response of 1.14 ± 0.23 and 0.98 ± 0.043 was obtained from 250 and 500 µm U-bent probes, respectively. Although the 250 µm POF probes gave rise to nearly 15% more response, they were too flexible to position them into microcentrifuge vials containing analyte and Gabs tightly. Because of this reason, a larger standard deviation of 20.2% was observed for 250 µm probes in comparison to 4.4% for 500 µm probes. Since the U-bent probes made of 500 µm POF were easy-to-handle, they were used in all subsequent studies.

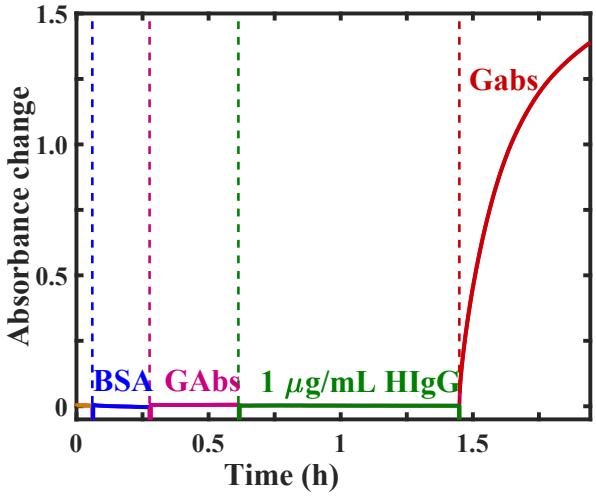

(a)

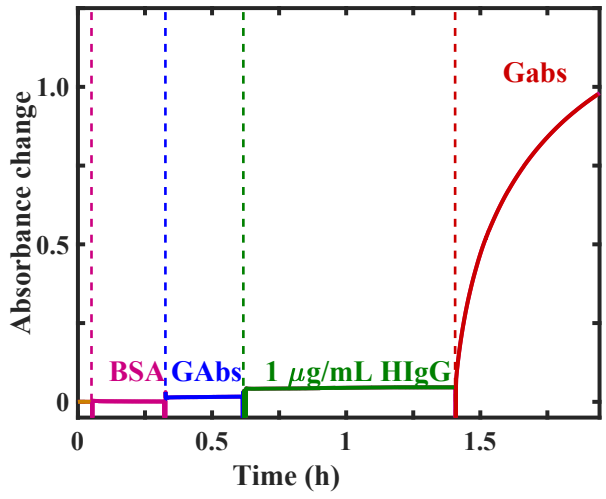

(b)

Figure 2: The real-time absorbance changes for HIgG detection using plastic optical fiber with a core diameter of (a) 250 µm and (b) 500 µm.

AuNP bioconjugation with anti-CHIKV-nsP3 antibodies

The anti-CHIKV-nsp3 polyclonal antibodies were developed in-house as described as elsewhere [13]. Conjugation of AuNP with the CHIKV-nsp3Ab involves an investigation of optimum dilution factor for the antibodies to be added to the AuNP solution as well as validation of the activity of AuNP-CHIKV-nsP3Ab conjugates.

An optimum concentration of CHIKV-nsP3Ab for AuNP conjugation maximizes the presence of active antigen-binding sites by enabling a suitable orientation of the antibodies on the AuNP surface [44]. To investigate an optimum concentration of CHIKV-nsP3Ab, several dilutions of the antibodies, including 1:50, 1:150, 1:300, 1:600, and 1:1000, were prepared and added to AuNP solution (100 µL in 1 mL respectively) to obtain the AuNP bioconjugates. UV-visible absorbance spectra were obtained from these preparations, as shown in Fig. 3a (normalized). Their spectral characteristics, including the peak wavelength shift and full width at half maxima (FWHM) of plasmonic resonance response, were compared with those of bare AuNP (Fig. 3b). When the dilution ratio was changed from 1:50 to 1:150, the red-shift in the peak wavelength (peak at 534 nm), as well as the FWHM, remained at 5 nm and 60 nm, respectively. On the other hand, beyond a dilution ratio of 1:150, an increase in these characteristics was observed.

The photographic images of the vials with AuNP-CHIKV-nsP3Ab conjugates for dilution of 1:300 and beyond showed a visible change in the color from pink to pale purple (inset in Fig. 3a). A red-shift is anticipated after antibody conjugation due to the difference in the local refractive index [45]. However, this is also possible with the aggregation of AuNP due to the insufficiency of antibodies to completely cover a given AuNP surface and bridging two or more AuNP [46]. These results reveal a possible agglomeration of an increasing fraction of the AuNP with dilution due to incomplete surface coverage by the antibodies. While 1:50 and 1:150 dilutions gave rise to similar peak shift and FWHM, lower antibody concentration is anticipated to provide a suitable side-on antibody orientation and a higher number of antigen-binding sites [44]. Hence, CHIKV-nsP3Ab dilution of 1:150 was chosen as an optimum concentration for AuNP bioconjugation.

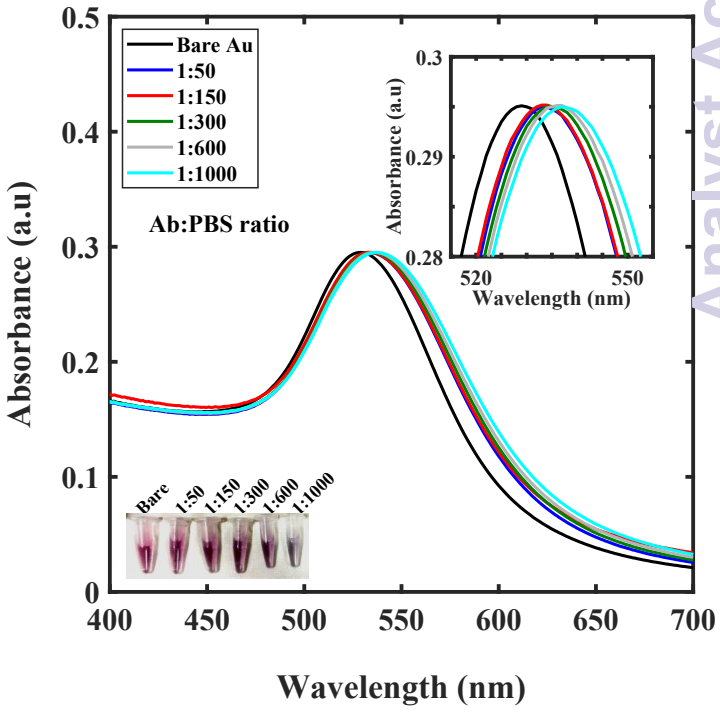

(a)

View Article Online
DOI: 10.1039/D0AN01603A

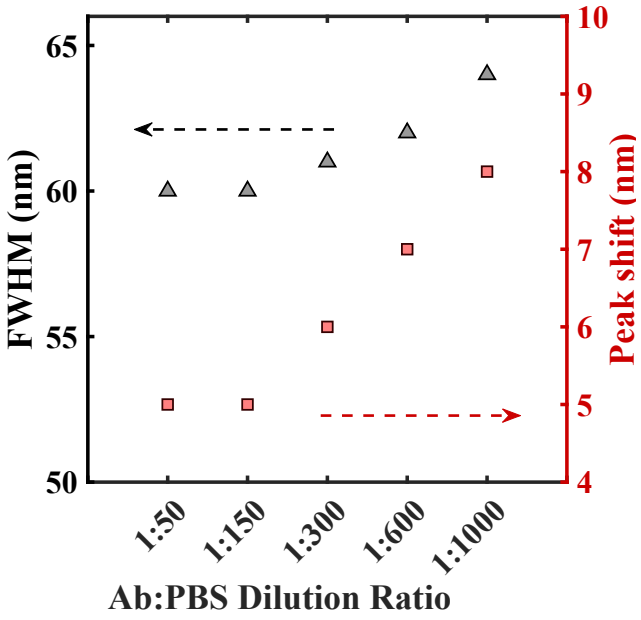

(b)

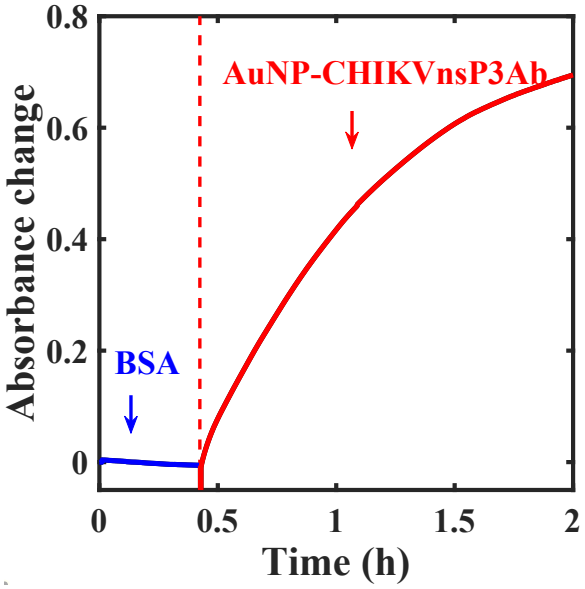

(c)

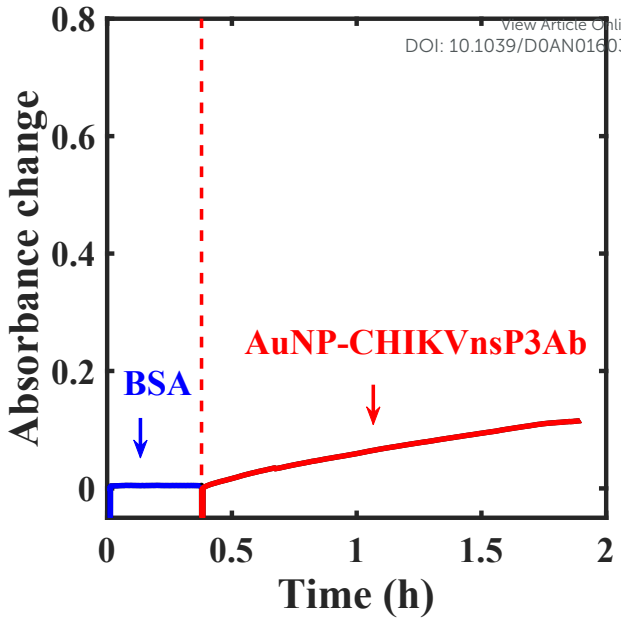

(d)

Figure 3. (a) UV-visible absorbance spectra (normalized) of conjugated antibodies (AuNP-CHIKVnsP3Ab) at various dilution ratios of CHIKV-nsP3Ab to PBS (b) Variation of peak shift and FWHM as a function of AuNP CHIKVnsP3Ab: PBS dilution ratio. Time-dependent absorbance response due to the binding of AuNP-CHIKVnsP3Ab on the U-bent fiber surface-functionalized with (c) CHIKV-nsP3 (Direct assay) and (d) BSA (Control for direct assay)

Subsequently, the binding affinity of AuNP-CHIKV-nsP3Ab towards CHIKV-nsP3 analyte was evaluated by realizing a direct assay as follows. The functionalized U-bent probes were immobilized with CHIKV-nsP3 by incubating them in 10 µg/mL of CHIKV-nsP3 overnight at 4 °C and washing them in PBS. The bio-functionalized probe was then exposed to 5 mg/mL BSA to block unbound sites. Then, the probe was incubated in the AuNP-CHIKV-nsP3Ab solution to realize direct assay. Figure 3c shows the transient absorbance response due to the binding of AuNP-CHIKV-nsP3Ab to the analyte on the U-bent POF probe surface. Upon exposure to Gabs, a significant increase in the absorbance response of ~ 0.72 ± 0.026 is seen. A control experiment was performed using a U-bent probe without the analyte on its surface. Instead of CHIKV-nsP3, the probe was incubated in BSA, and then, it was exposed to AuNP-CHIKVnsP3Ab, and the results are shown in Figure 3d. A small change in absorbance (~0.12 ± 0.01) attributed to non-specific binding was observed from the control probe. With these results, we could confirm the activity of AuNP-CHIKV-nsP3Ab conjugates towards CHIKV-nsP3 analyte detection.

Realization of Plasmonic POF immunobiosensor

A proof-of-concept U-bent POF based plasmonic sandwich immunosensor was realized using a compact set-up consisting of a green LED and a photodetector. Figure 4a shows the absorbance

response obtained in real-time from a 500 µm U-bent POF probes functionalized with poly-histidine antibodies incubated in 5 mg/mL BSA solution, followed by the CHIKV-nsP3 (10 µg/mL) sample solution and AuNP-CHIKV-nsP3Ab solution for 2 hrs and 1.5 hrs respectively. No considerable change in the sensor absorbance response was observed during incubation in BSA and analyte solutions. A significant increase in the response was observed as soon as the CHIKV-nsP3 bound probes are exposed to AuNP-CHIKV-nsP3Ab due to the rapid formation of the sandwich immunocomplex with AuNP labels on the probe surface. Absorbance values as large as 0.62 ± 0.03 (a.u.) were obtained. In a control experiment, where the capture antibody functionalized U-probes were directly exposed to AuNP-CHIKV-nsP3Ab without incubating in the CHIKV-nsP3 sample solution, a peak absorbance of ~0.113 ± 0.004 was observed. It indicates considerable non-specific adsorption of 18% of the antigen-binding, similar to that obtained in Figure 3c. These results corroborate with the earlier reported study [37]. The SEM image of the probe, shown in Fig. 4b confirms the presence of AuNP on the probe surface.

Subsequently, sensor response for various concentrations of the analyte ranging from 0.1 to 10000 ng/mL was obtained, as shown in Figure 5a. The absorbance values obtained for 0.1 ng/mL were almost close to that of control, i.e., without the analyte. Figure 5b shows the dose-response curve for the CHIKV-nsP3 concentrations between 1 ng/mL and 10^4 ng/mL. The horizontal red line in Figure 5b corresponds to the mean of the blank sample response ± three times the standard deviation. The absorbance response was linear over the complete range of the analyte concentrations investigated in this study. In this range, the relationship between the sensor absorbance response (A_{530nm}) and CHIKV-nsP3 concentration (C_{nsP3}) was obtained as $\Delta A_{530nm} = 0.1043 \log_{10}(C_{nsp3}) + 0.155$; R^2 = 0.98, where C_{nsP3} is in ng/mL. The LOD, calculated as the sum of the mean value of the blank signal and thrice the standard deviation [47], was found to be 0.52 ng/mL. On the other hand, the smallest concentration that can be practically quantified, denoted by the limit of quantification (LOQ), is defined as the sum of the blank signal and ten times the standard deviation [47]. The LOQ was found to be 0.96 ng/mL, which is close to the experimentally observed concentration of the sample, which yielded a signal that is clearly distinguishable from the blank signal, viz. 1 ng/mL.

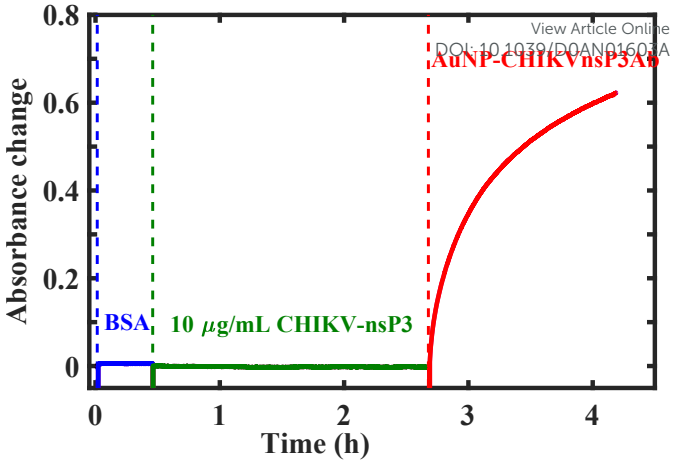

(a)

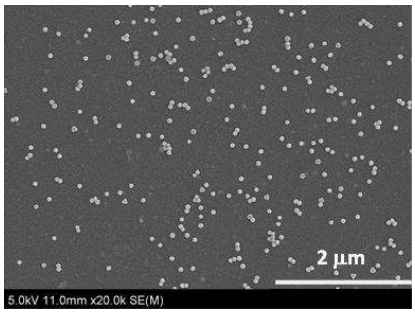

(b)

Figure 4. (a) Temporal response showing binding kinetics of AuNP-CHIKVnsP3Ab on U-bent fiber surface exposed to 10 µg/mL CHIKV-nsP3 obtained using LED-PD set-up. (b) HR-SEM image of a U-bent POF probe showing the AuNP labels.

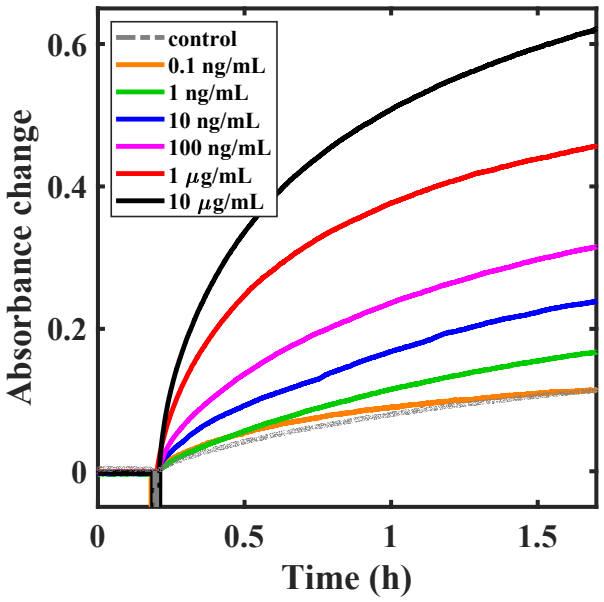

(a)

View Article Online
DOI: 10.1039/D0AN01603A

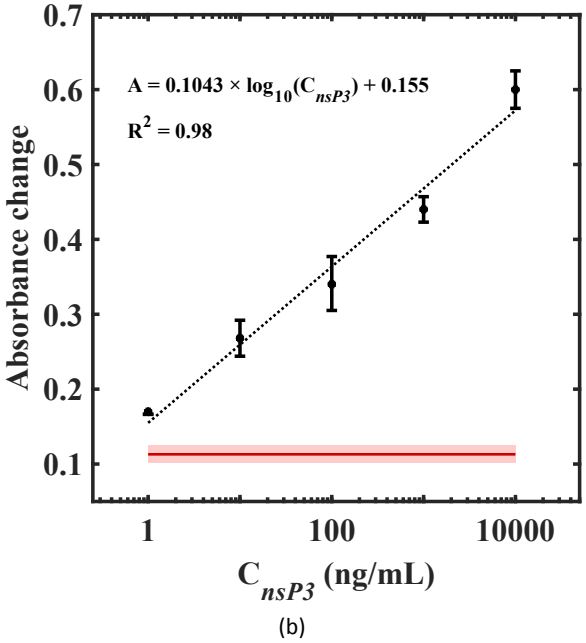

Figure 5. Temporal response showing binding kinetics of AuNP-CHIKVnsP3Ab on fiber surface exposed to different concentrations of the analyte from 0.1 ng/mL to 10 µg/mL. (b) Dose-response curve for plasmonic fiber optic sandwich immunobiosensor. The concentration is shown in logarithmic scale. The horizontal line signifies the sum of the average of the control signal and thrice the standard deviation.

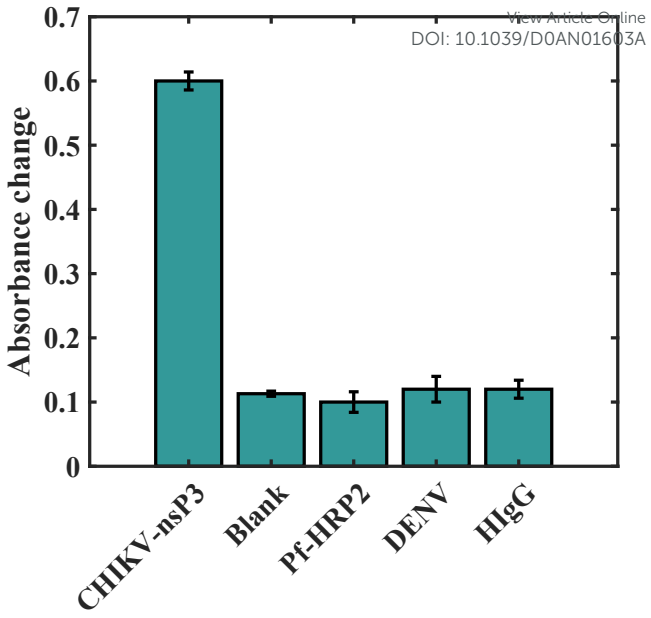

Figure 6. Absorbance response for 10 µg/mL CHIKV-nsP3 compared to blank and other bioanalytes:10 µg/mL of Pf-HRP2, DENV, and HIgG.

Specificity of the immunobiosensor

The specificity of the developed immunobiosensor was evaluated by comparing absorbance changes for 10 µg/mL CHIKV-nsP3 with other bio-analytes at the same concentration, and the results are presented in Figure 6. The absorbance changes for 10 µg/mL of CHIKV-nsP3 was 0.62 ± 0.03, whereas blank sample, HIgG, Pf-HRP2 and DENV yielded an absorbance response of 0.113 ± 0.004, 0.1 ± 0.06, 0.12 ± 0.02 and 0.12 ± 0.014, respectively. These results indicate that the proposed sensor demonstrates appreciable specificity towards CHIKV-nsP3.

One of the best validations is the utility of any technique in detecting a specific analyte in patient samples. In real patient sera, interference from other molecules can cause problems, and further modifications to the protocol may be necessary to achieve specific detection of nsP3 with a LOD of 1 ng/mL. In the case of arboviral infections such as chikungunya, the viral titers can reach as high as 10^9 genome copies per mL in the infected blood [48]. In the case of dengue, studies have shown that LOD could be as low as 0.07 ug/mL of NS1 proteins in infected patient sera[49]. In the case of chikungunya, the presence of a massive amount of viral proteins, including those of CHIKV-nsP3 in patient sera, supports the use of this protein for diagnosis purposes[50]. In the present study, the POF based biosensor exhibited a LOD of ~ 1 ng/mL of nsP3, whereas traditional techniques such as Western blot and ELISA have LOD of 10 and 1 ng/mL of nsP3, respectively[13], making the sensitivity of the POF based biosensor comparable to that of ELISA[13].

The LOD obtained with the labeled technique in optical biosensor (0.52 ng/mL) is much lower compared to that of the label-free detection of the same biomarker using impedance biosensor (8 ng/mL) and quartz crystal microbalance (500 ng/mL) [13]. The enhancement of the optical signal by the AuNP-CHIKVnsP3Ab labels results in a lower LOD compared to the label-free detection techniques. Apart from that, optical-based sensing is known to be electrically passive compared to the other two biosensing techniques [21, 51], and appears to be the most promising among the three.

Conclusions

As the conventionally available methods for the detection of chikungunya are laboratory-based and time-consuming, an EWA based U-bent POF was proposed for the detection of one of its viral proteins, CHIKV-nsP3. A sandwich immunoassay with 40 nm AuNP as labels was performed using the immunobiosensor with CHIKV-nsP3 as the detection analyte. A significant change in absorbance response for analyte bound probes was observed in comparison to the control, and SEM confirmed the binding of the labeled secondary antibody to the probe. We evaluated the relevant sensor parameters of the immunobiosensor, and the LOD was 0.52 ng/mL, and the sensitivity was 0.1043 $A_{530nm}/\log(C_{nsP3})$. The developed immunosensor also showed appreciable specificity. The results demonstrate the potential of EWA based U-bent POFs as an excellent alternative to both conventional diagnostic methods and label-free biosensors, for the early detection of chikungunya viral disease.

In this proof-of-the-concept study, the CHIKV-nsP3 analyte is His-tagged mainly to aid in the purification of the protein, and it is absent in the real serum samples. Hence, the sandwich assay may involve polyclonal antibodies against CHIKV-nsP3 as capture antibody instead of anti-polyhistidine antibodies utilized to illustrate these feasibility studies. Given the design of plasmonic fiber optic sandwich immunosensor demonstrated here, a monoclonal antibody against CHIKV-nsP3 may be utilized to conjugate AuNP for highly specific detection of chikungunya infection.

Conflicts of interest

The authors declare no conflict of interest

Acknowledgments

Financial support provided by the Department of Biotechnology, Ministry of Science and Technology (DBT), India in the project BT/PR11837/MED/32/347/2014, is gratefully acknowledged.

References

1. S. Vigneshvar, C. C. Sudhakumari, B. Senthilkumaran and H. Prakash, *Frontiers in bioengineering and biotechnology*, 2016, **4**, 11.
2. M. S. Cheng and C. S. Toh, *The Analyst*, 2013, **138**, 6219-6229.
3. A. P. Turner, *Chemical Society reviews*, 2013, **42**, 3184-3196.
4. G. Zanchetta, R. Lanfranco, F. Giavazzi, T. Bellini and M. Buscaglia, *Nanophotonics*, 2017, **6**, 627-645.
5. B. Pejcic, R. De Marco and G. Parkinson, *The Analyst*, 2006, **131**, 1079-1090.
6. A. Syahir, K. Usui, K. Y. Tomizaki, K. Kajikawa and H. Mihara, *Microarrays*, 2015, **4**, 228-244.
7. M. L. Sin, K. E. Mach, P. K. Wong and J. C. Liao, *Expert review of molecular diagnostics*, 2014, **14**, 225-244.
8. L. Baril, *Handbook of Biosensors and Biochips*, 2008.
9. J. Jain, K. Nayak, N. Tanwar, R. Gaind, B. Gupta, J. S. Shastri, R. K. Bhatnagar, M. K. Kaja, A. Chandele and S. Sunil, *Clinical infectious diseases : an official publication of the Infectious Diseases Society of America*, 2017, **65**, 133-140.
10. N. Kaur, J. Jain, A. Kumar, M. Narang, M. K. Zakaria, A. Marcello, D. Kumar, R. Gaind and S. Sunil, *New microbes and new infections*, 2017, **20**, 39-42.
11. V. Londhey, S. Agrawal, N. Vaidya, S. Kini, J. Shastri and S. Sunil, *J Assoc Physicians India*, 2016, **64**, 36-40.
12. J. Jain, T. Okabayashi, N. Kaur, E. Nakayama, T. Shioda, R. Gaind, T. Kurosu and S. Sunil, *Virology journal*, 2018, **15**, 84.
13. A. George, M. S. Amrutha, P. Srivastava, V. V. R. Sai, S. Sunil and R. Srinivasan, *Journal of The Electrochemical Society*, 2019, **166**, B1356-B1363.
14. T. Okabayashi, T. Sasaki, P. Masrinoul, N. Chantawat, S. Yoksan, N. Nitatpattana, S. Chusri, R. E. M. Vargas, M. Grandadam and P. T. Brey, *Journal of clinical microbiology*, 2015, **53**, 382-388.
15. A. Singh, A. Kumar, R. Yadav, V. N. Uversky and R. Giri, *Scientific reports*, 2018, **8**, 5822.
16. M. E. Álvarez-Argüelles, S. R. Alba, M. R. Pérez, J. A. B. Riveiro and S. M. García, in *Current Topics in Neglected Tropical Diseases*, IntechOpen, 2019.
17. C. Singhal, A. Dubey, A. Mathur, C. S. Pundir and J. Narang, *Process Biochemistry*, 2018, **74**, 35-42.
18. C. Singhal, M. Khanuja, N. Chaudhary, C. S. Pundir and J. Narang, *Scientific reports*, 2018, **8**, 7734.
19. C. Chen and J. Wang, *The Analyst*, 2020, **145**, 1605-1628.
20. E. Benito-Pena, M. G. Valdes, B. Glahn-Martinez and M. C. Moreno-Bondi, *Analytica chimica acta*, 2016, **943**, 17-40.
21. G. Liang, Z. Luo, K. Liu, Y. Wang, J. Dai and Y. Duan, *Critical reviews in analytical chemistry*, 2016, **46**, 213-223.
22. H. Usman, M. H. Abu Bakar, A. S. Hamzah and A. b. Salleh, *Sensor Review*, 2016, **36**, 40-47.
23. M. E. Bosch, A. J. R. Sanchez, F. S. Rojas and C. B. Ojeda, *Sensors*, 2007, **7**, 797-859.
24. M. Divagar, A. Gowri, S. John and V. V. R. Sai, *Sensors and Actuators B: Chemical*, 2018, **262**, 1006-1012.
25. N. Cennamo, S. Di Giovanni, A. Varriale, M. Staiano, F. Di Pietrantonio, A. Notargiacomo, L. Zeni and S. D'Auria, *PloS one*, 2015, **10**, e0116770.
26. A. Gowri and V. V. R. Sai, *Sensors and Actuators B: Chemical*, 2016, **230**, 536-543.
27. N. Cennamo and L. Zeni, *Macromolecular Symposia*, 2020, **389**, 1900074.
28. D. Marazuela and M. C. Moreno-Bondi, *Analytical and bioanalytical chemistry*, 2002, **372**, 664-682.
29. R. Bharadwaj, V. V. Sai, K. Thakare, A. Dhawangale, T. Kundu, S. Titus, P. K. Verma and S. Mukherji, *Biosensors & bioelectronics*, 2011, **26**, 3367-3370.
30. V. V. Sai, T. Kundu and S. Mukherji, *Biosensors & bioelectronics*, 2009, **24**, 2804-2809.
31. G. Wandermur, D. Rodrigues, R. Allil, V. Queiroz, R. Peixoto, M. Werneck and M. Miguel, *Biosensors & bioelectronics*, 2014, **54**, 661-666.
32. G. Liang, Z. Zhao, Y. Wei, K. Liu, W. Hou and Y. Duan, *RSC Advances*, 2015, **5**, 23990-23998.

View Article Online
DOI: 10.1039/D0AN01603A

33. A. Leung, P. M. Shankar and R. Mutharasan, *Sensors and Actuators B: Chemical*, 2007, **125**, 688-703.
34. T. Gessei, T. Arakawa, H. Kudo and K. Mitsubayashi, *The Analyst*, 2015, **140**, 6335-6342.
35. Z. Huang, X. Lei, Y. Liu, Z. Wang, X. Wang, Z. Wang, Q. Mao and G. Meng, *ACS Applied Materials & Interfaces*, 2015, **7**, 17247-17254.
36. Y. Liu, Z. Huang, F. Zhou, X. Lei, B. Yao, G. Meng and Q. Mao, *Nanoscale*, 2016, **8**, 10607-10614.
37. B. Ramakrishna and V. V. R. Sai, *Sensors and Actuators B: Chemical*, 2016, **226**, 184-190.
38. M. Gandhi, S. Chu, K. Senthilnathan, P. Babu, K. Nakkeeran and Q. Li, *Applied Sciences*, 2019, **9**, 949.
39. C. Nietzold and F. Lisdat, *The Analyst*, 2012, **137**, 2821-2826.
40. R. N. Lopes, D. M. C. Rodrigues, R. C. S. B. Allil and M. M. Werneck, *Measurement*, 2018, **125**, 377-385.
41. M. Divagar and V. V. R. Sai, *IEEE sensors conference proceedings*, 2018, 1-4.
42. J. Turkevich, P. C. Stevenson and J. Hillier, *Discussions of the Faraday Society*, 1951, **11**, 55.
43. C. G. Danny, M. D. Raj and V. V. R. Sai, *JOURNAL OF LIGHTWAVE TECHNOLOGY*, 2020, **38**, 1580-1588.
44. B. Saha, T. H. Evers and M. W. Prins, *Analytical chemistry*, 2014, **86**, 8158-8166.
45. K. Tripathi and J. D. Driskell, *ACS omega*, 2018, **3**, 8253-8259.
46. R. T. Busch, F. Karim, J. Weis, Y. Sun, C. Zhao and E. S. Vasquez, *ACS omega*, 2019, **4**, 15269-15279.
47. J. Mocak, A. M. Bond, S. Mitchell and G. Scollary, *Pure and Applied Chemistry*, 1997, **69**, 297-328.
48. S. C. Weaver and M. Lecuit, *New England Journal of Medicine*, 2015, **372**, 1231-1239.
49. P. R. Young, P. A. Hilditch, C. Bletchly and W. Halloran, *Journal of clinical microbiology*, 2000, **38**, 1053-1057.
50. Y. W. Kam, F. M. Lum, T. H. Teo, W. W. Lee, D. Simarmata, S. Harjanto, C. L. Chua, Y. F. Chan, J. K. Wee, A. Chow, R. T. Lin, Y. S. Leo, R. Le Grand, I. C. Sam, J. C. Tong, P. Roques, K. H. Wiesmuller, L. Renia, O. Rotzschke and L. F. Ng, *EMBO molecular medicine*, 2012, **4**, 330-343.
51. R. Verma and B. D. Gupta, *The Analyst*, 2013, **138**, 7254-7263.